university of groningen

Uncertainty assessment of count rate measurements in respect to potential anti-neutrino induced decay constant variation

Bachelor Thesis

Jonah Noble
S2712644

Examiners

First examiner: Emiel van der Graaf

Second examiner: Catherine Rigollet

Contents

1. Introduction

Since the discovery of the radioactive decay law by Ernest Rutherford, (Rutherford, Chadwick, Ellis, 1931) it has been considered that the decay constants of radionuclides are constant under all conditions. This results in the exponential decay law, $N = N_0 e^{-\lambda t}$, where λ represents a decay constant specific to the radionuclide, *N* represents the number of nuclei at time *t* and N_0 the starting number of nuclei. When differentiated with respect to time this formula gives the decay rate as $\frac{dN}{dt} = -\lambda N_0 e^{-\lambda t} = -\lambda N(t)$.

This displays how the decay rate of a radionuclide sample depends only on the decay constant and the number of nuclei remaining in the sample. The decay constant has the units of s^{-1} and represents the inverse of the mean lifetime of an atom of the specific radionuclide it describes. The mean lifetime is used as the process of radioactive decay is random making it impossible to predict the exact time at which a nucleus will decay.

This invariance in decay constants has been utilised to date items through radioactive dating, the most well-known example is using ^{14}C, which provides results verifiable by alternative dating methods. This provides evidence pointing towards invariable decay constants. In addition, radionuclide half-lives given by $t_{\frac{1}{2}} = \frac{\ln(2)}{\lambda}$, when measured independently have been found to converge to specific values (DDEP, 2017) which again provides evidence for the invariance of λ in time and space.

A recent study found correlations between the decay constants of ^{32}Si and ^{226}Ra and the distance from the sun (Jenkins et al 2009). For such counting experiments one nuclide sample is compared with a long-lived standard. The standard is measured in the same detector in order to minimise the impact of systematic effects and to give a stable rate for comparison. In the Jenkins (2009) study the decay of ^{36}Cl was used as a long-term comparison standard for ^{32}Si and ^{152}Eu and ^{154}Eu were compared to ^{226}Ra. The data for each of the samples was collected in different locations with the ^{32}Si half-life being measured at Brookhaven National Laboratory in the United States and the ^{152}Eu, ^{154}Eu and ^{226}Ra decays were measured at the Physikalisch-Technische-Bundesanstalt in Germany (Jenkins et al, 2009). These measurements were analysed and found a strong correlation of both the $^{32}Si/^{36}Cl$ ratio and the ^{226}Ra with $\frac{1}{R^2}$ where *R* is the earth-sun distance in astronomical units. The decay rate ratios were found to vary by 0.2% in relation to a variation in $\frac{1}{R^2}$ of 0.2-0.3%. After background corrections, which included removing the seasonally variant ^{222}Rn background and averaging thirty individual data points, the ^{226}Ra decay data was found to have a similar relationship. However, this was no longer observed when the ratio of $Eu/^{226}$ Ra decay rates was used. This correlation could be due to a variety of different variables related to the earth-sun distance such as seasonal temperature, another theory is the potential influence of neutrinos from the sun. This is due to the solar neutrino flux also varying with $\frac{1}{R^2}$. Another study also found perturbations in the decay rate of ^{54}Mn during solar flares (Jenkins, Fischbach, 2009). Neutrinos are favoured as there is still a lack of understanding of their behaviour and interactions.

These findings have been disputed multiple times. Pomme et al (2018) analysed different radionuclides with different decay schemes over a variety of time frequencies coinciding

with solar activity cycles. This analysis included 12 data sets each corresponding to a different radionuclide with differing decay processes including α decay, both β^+ and β^- decays and electron capture. This data was also taken from 4 different metrology institutes and was also compared to the neutrino flux data taken from the Super-Kamiokande in Japan. The data used included the following radionuclides, ^{3}H, ^{14}C, ^{90}Sr, ^{134}Cs, ^{152}Eu, ^{22}Na, ^{54}Mn, ^{65}Zn, ^{109}Cd ^{209}Po, ^{226}Ra and ^{241}Am. The analysis found no common oscillations between the radionuclides and states there is no evidence that the decay rates are influenced by neutrino flux. Although fluctuations were found they were less than three times the uncertainties of the measurements, which were between 0.00023-0.023% for all twelve radionuclides analysed. ^{134}Cs had the lowest uncertainty and ^{3}H the highest.

To find whether anti-neutrinos influence nuclear decay constants a highly accurate ratio of decay rates between two sources is required. Antineutrinos are chosen as solar neutrinos are highly non-interacting therefore shielding a sample would prove difficult whereas the flux of reactor produced antineutrinos is more localised and therefore easier to minimise the flux the comparison source experiences. In this investigation two radioactive sources would be required. These sources should be as similar as possible in order to detect the potential changes caused. These samples would both have a long-term measurement in which its decay rate is taken and the ratio of the decay rates of the two samples will be calculated. These long-term measurements will need to be in the same detector in order to keep the conditions as close as possible. Once the ratio of count rates has been established one of the samples will be placed in the vicinity of a nuclear reactor which will expose the sample to an elevated anti-neutrino flux. The samples will then undergo the same long-term decay rate measurement, again in the same detector, and a new ratio of count rates will be found. This new ratio can then be compared to the pre-exposure ratio in order to see if the exposure caused any variation to the decay constant.

The purpose of this thesis is to measure the ratio of count rates and find the maximum accuracy possible with the equipment available. Following this introduction there is a brief outline of the theory behind the interactions of gamma radiation with matter as well as the theory behind gamma spectroscopy. It goes on to describe the method used for this investigation followed by the results, discussion and conclusion.

2. Theory

2.1 Interactions of gamma radiation with matter

Gamma radiation consists of high frequency photons emitted from unstable nuclei with excess energy. Due to the high energy and lack of mass, gamma radiation is a very penetrating form of nuclear radiation. Gamma radiation interacts with matter via three main methods, the photoelectric effect, Compton scattering and pair production.
At lower energies the photoelectric effect dominates. The photoelectric effect is caused by the absorption of the photons energy by a bound electron. If the energy transferred exceeds the binding energy of the electron the electron is emitted with the remainder of the photons energy. One of the remaining bound electrons may transition to fill the now empty energy level or the atom can take part in electron capture. This electron energy level transition can lead to x-ray emission.
Compton scattering dominates at the intermediate energies of gamma radiation. Compton scattering is when a high energy photon is scattered by an electron transferring some of its energy to the electron reducing the energy of the photon depending on the angle of deflection with the change in energy given by $\Delta\lambda=\lambda'-\lambda=\frac{h}{m_e c}(1-cos\theta)$ with λ being the wavelength of the gamma photon, *h* the planck constant, *c* the speed of light and m_e being the mass of an electron. If a photon has a deflection angle of 180 degrees and escapes it transfers the maximum possible energy into the electron, this causes a 'Compton edge' (see figure 1) in the spectrum with a 'Compton plateau' to its left. If sufficient energy is transferred the deflected electron can act as a beta particle and can proceed to collide with other electrons to cause further ionisations.

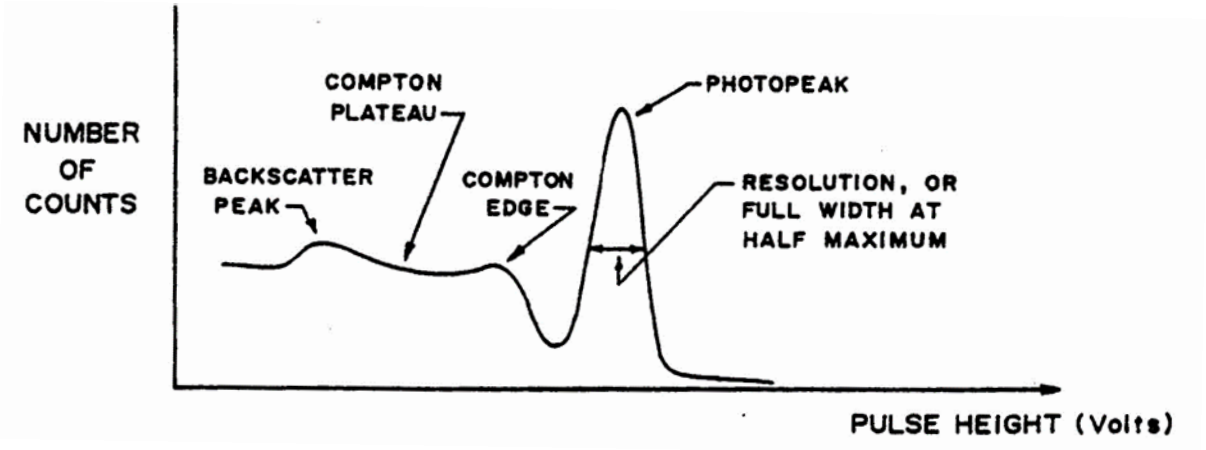

Figure 1 A ^{137}Cs gamma spectrum with typical features of a gamma spectrum labelled (physwiki)

The third interaction of gamma photons is pair production, where the photons energy is converted into the production of an electron and positron pair. Pair production is an exclusively high energy phenomena and requires photons with an energy of above 1022 keV. This energy corresponds to two times the rest mass of an electron, any energy above this is then shared between the two particles as kinetic energy. This particle creation is unable to take place in free space as it would violate the conservation of both energy and momentum, so it has to take place near a nucleus in order to balance the energies. When a

positron and electron interact within the detector they annihilate and emit a photon at 511 keV, known as annihilation radiation.

2.2 Theory behind gamma spectroscopy

Gamma spectroscopy is the process of quantifying or identifying radionuclides from their gamma spectrums. The spectrometer provides both the quantity and energies of the gamma emissions, with the amplitude representing the activity of the sample and the position on the horizontal axis representing the energies. Gamma spectrometers typically use a semiconductor crystal to detect the radiation, usually germanium or silicon, set between a high voltage. This creates three areas in the crystal positive, intrinsic and negative where the intrinsic area is the area sensitive to radiation.

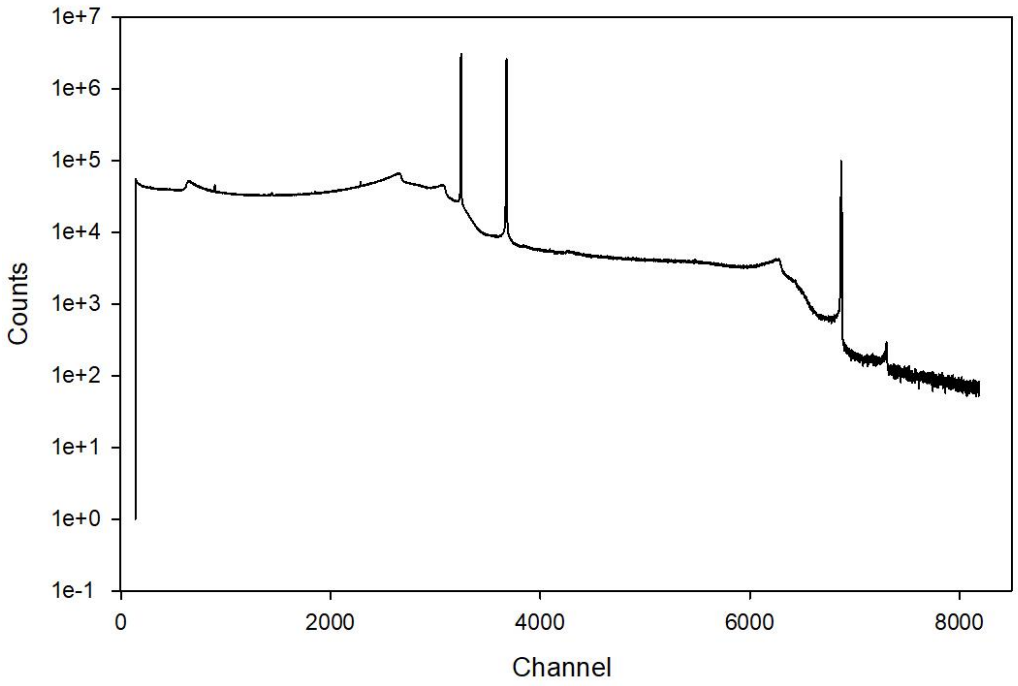

Fig 2 Typical gamma spectrum of ^{60}Co

When charged particles or radiation interact with the semiconductor crystal in the intrinsic region of the crystal, electrons are given enough energy to move from the valence band to the conduction band. These electrons are then carried by the voltage to the positive electrode which creates an electrical current. The movement of the electron also creates a 'hole' which get filled by adjacent electrons, this hole eventually travels to the negative electrode where it also forms a current. This current then forms the signal which is sent to the preamplifier. These signal pulses are further amplified and shaped into peaks before being converted into a numerical digital signal. This digital signal is sent to a multi-channel analyser which then proceeds to send the resultant spectrum to a computer where the spectrum is visualised. The multi-channel analyser is required as the channel where the count is detected relates to a specific energy. The total charge of the carriers in an individual pulse is proportional to the energy of the incoming photon which in turn affects the size of the voltage pulse enabling the energy of the photon to be measured. Due to the way the detector works there is also a short dead time between detections where any photons that

interact with the crystal are unable to be processed and therefore are not included in the spectra.

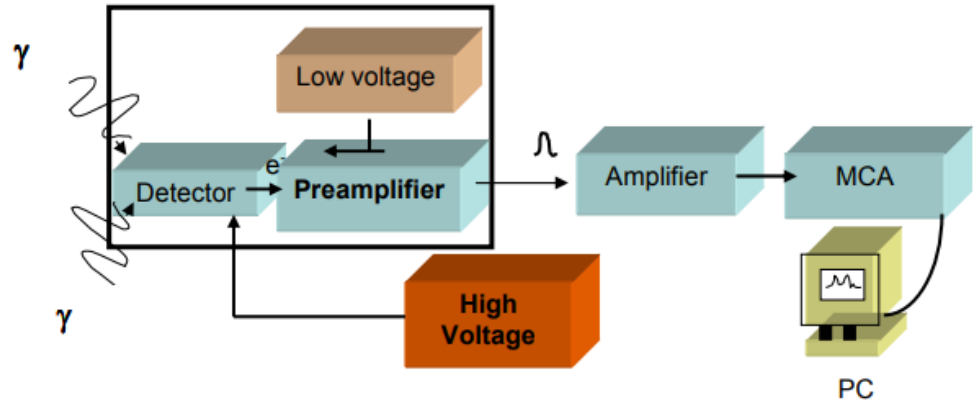

Figure 3 Basic gamma spectrometer set up (Nafaa Reguigui 2006)

Some detector crystals need to be doped with other atoms in order to increase sensitivity and to prevent any charge carriers from being trapped due to insufficient purity. With Germanium detectors it is also important to keep them at very low temperatures to prevent the production and detection of thermally excited charge carriers. This is typically done using liquid nitrogen, with a metal rod being placed in the liquid nitrogen and the other end having the detector material placed upon it within a vacuum container. This method ensures the detector is cooled with the vacuum also preventing any condensation from forming in the detector.

3. Method

3.1 ^{60}Co

For this experiment a sample of ^{60}Co is being used. ^{60}Co is a radioactive isotope of Cobalt with 27 protons and 33 neutrons and a half-life of 5.2712 years. ^{60}Co decays via beta minus and gamma emissions to Nickel.

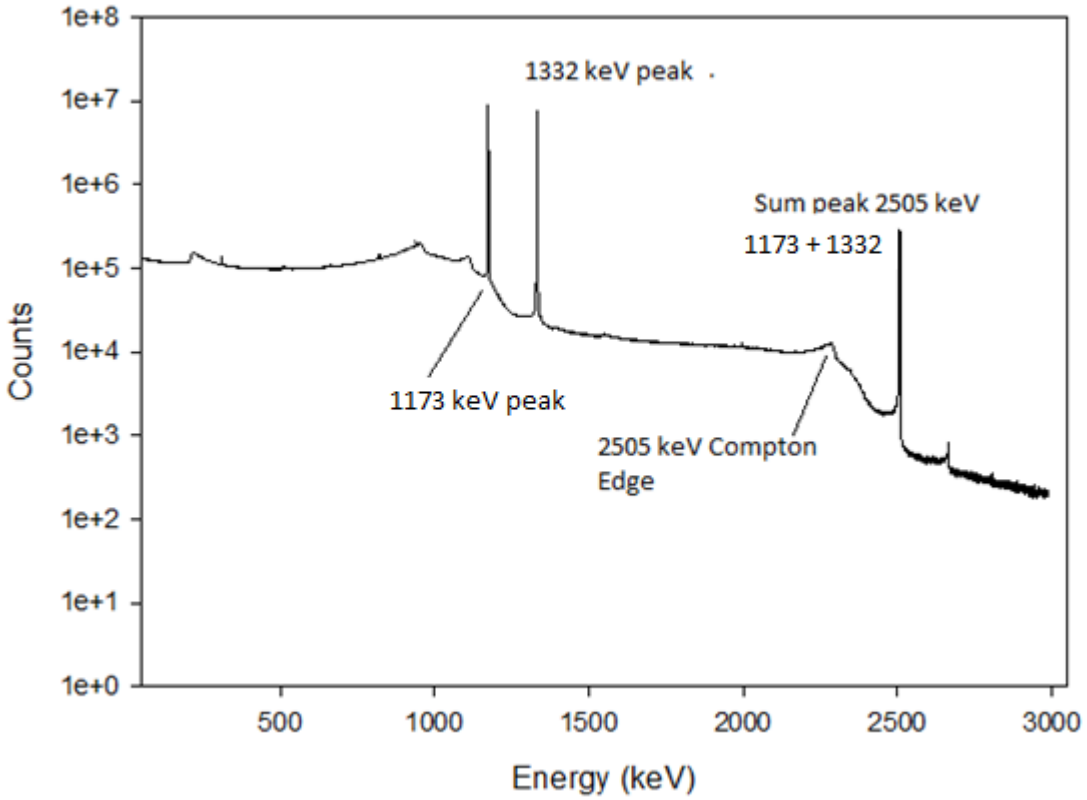

Figure 4 Energy calibrated gamma spectrum of ^{60}Co

As seen in figure 4, the decay scheme of ^{60}Co has two main Gamma photo peaks at 1173 keV and 1332 keV respectively. It is also possible for both of these photons to be detected simultaneously which forms another peak at 2505 keV known as the sum peak. All of these peaks correspond to a full deposition of the decay energy so are classed as full energy peaks (FEP). To the left of each of these photo peaks there is a range of energies with reduced counts, known as a Compton plateau followed by a Compton edge which are created via the Compton scattering of the radiation.

If a photon with an energy of above 1022 keV is emitted a positron electron pair can be produced. If the positron interacts with an electron and annihilates it will emit a photon, if one of these photons escapes a peak will be produced at 511 keV below the full energy peak, or if both photons escape, 1022 keV below. If one of these photons is detected it will produce a 511 keV peak in the spectrum.

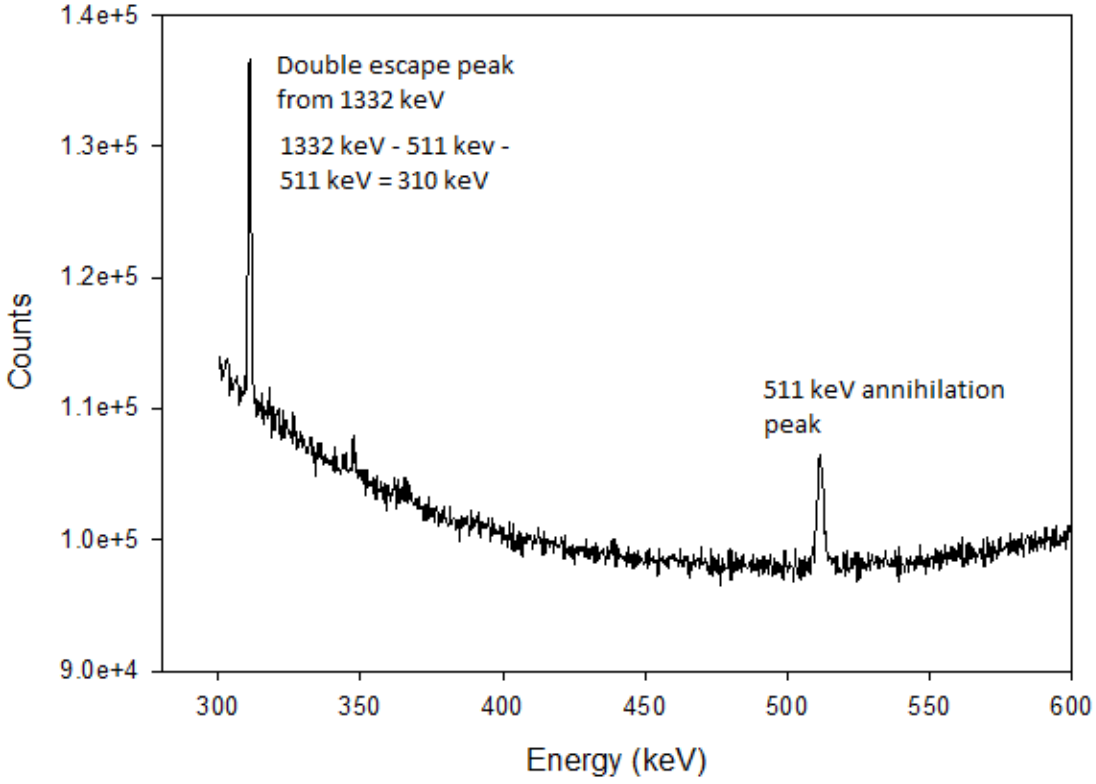

Figure 5 Close up of the ^{60}Co spectra from 300-600 keV showing the double escape peak from 1332 keV full energy peak and the 511 keV annihilation peak.

Figure 5 shows a peak at approximately 310 keV and corresponds to a double escape peak of the 1332 keV gamma photon. The double escape peak is caused by the escape of the two photons produced by the annihilation of an electron and positron which both escape the detector. The remaining energy of the initial photon is then deposited in the detector. The figure also shows the annihilation peak at 511keV which is created when a positron and electron interact and annihilate within the source, this emits a 511 keV photon which is detected in the spectrometer.

4. Method

For this experiment a ^{60}Co source with an original activity of 370 kBq is placed inside a high purity Germanium (HPGe) gamma spectrometer. The spectra are viewed in the PCA3 software and are exported to Microsoft Excel for analysis and Sigma Plot for graphing. Using a batch file, the detector acquired a spectrum per hour over a seven-day period overall providing 168 spectra. This gives a view on whether the time of day or day of the week has an impact on the decay rate observed. This aids the determination of variables that could impact the decay rates and if there could be alternative reasons for the patterns found in the other studies. A measurement is taken without a sample inside to obtain the background of the system. The measurements are repeated with the sample at different alignments within the detector to investigate whether the decay rate could be influenced by the positioning of the sample within the detector. These measurements are taken twice in order to calculate the accuracy achievable with this experimental setup. This should also

ensure the sample is under the same conditions for each measurement and minimising any systematic effects.
Each channel of the detector corresponds to a specific energy value of radiation given by the following formula

$$Energy = a_0 + a_1C + a_2C^2 + a_3C^3$$

where C is the channel number and
a_0= -1.71
a_1= 0.367
a_2= 6.78×10^{-9}
a_3= 1.17×10^{-12}
These coefficients were supplied by previous users of the spectrometer.
By using the decay scheme of ^{60}Co (see figure 6) it is possible to match each peak of the spectra with a decay path, this enables the total number of decay events to be calculated. As counts above certain energies actually correspond to multiple decays it is necessary to multiply some counts in order to calculate the total number of decays counted.

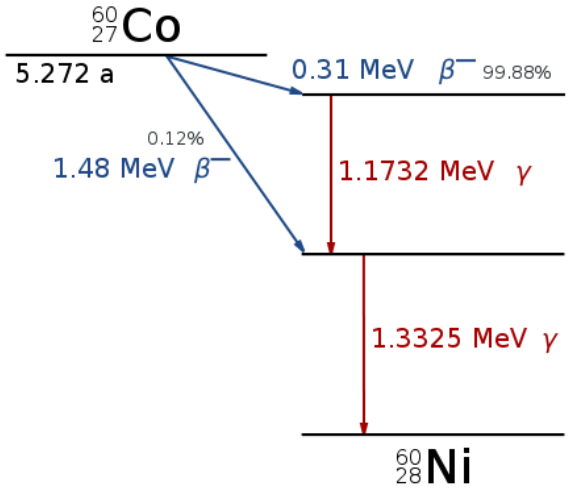

Figure 6 Decay Scheme of ^{60}Co (Nucleonica)

The lowest energy decay from ^{60}Co is a beta decay at 314 keV. X-ray energies range from 100 eV to 100 keV so detections in this range are ignored as are all other low energy detections below 240 keV. All detections from 240- 1332 keV are assumed to count as a single event. Beyond 1332 keV up until 2505 keV can be assumed to correspond to the simultaneous detection of 2 decay events. Above the energy of the sum peak the energies can only possibly be due to 3 events. The detections are then multiplied by the number of decays the energy corresponds to and then summed to get the total count rate. This data is then grouped into days or times in order to compare whether the decay rate changes throughout the day or daily throughout a week.
To analyse the data from the detector it is transferred to Microsoft Excel and the counts per second of each channel are calculated, this is also done for a long-term background measurement which is then subtracted from the source spectra which gives a total number of counts per second for the source. The background measurement has a count rate of 1.22±0.004 counts per second and the mean source count rate was found to be 2137.7±0.16.

5. Results

5.1 Daily Variability

In order to analyse the daily number of events the total number of decays from each of the 24-hourly spectra were added together. The number of counts per second were calculated for the hourly spectra as well as for the entire day. The table below shows the average count rate for each day and the error attributed to the count rate. As the decay is a Poisson distribution the error for the decay rates were calculated using the following equation $\sigma = \frac{\sqrt{Total\ Decays}}{Live\ time}$. Where the live time is the length of time over which the measurement was taken not including the dead time of the detector. For this measurement the background radiation detected would amount to 7.5σ or 0.53% increase in the count rate so can be seen to be statistically significant.

Table 1 Table of total daily count rates and uncertainty

Day	Total Count Rate	Uncertainty	Relative Uncertainty (%)
Monday	2137.47	0.16	0.008
Tuesday	2139.18	0.16	0.008
Wednesday	2138.68	0.16	0.008
Thursday	2137.72	0.16	0.008
Friday	2137.59	0.16	0.008
Saturday	2137.36	0.16	0.008
Sunday	2136.07	0.16	0.008

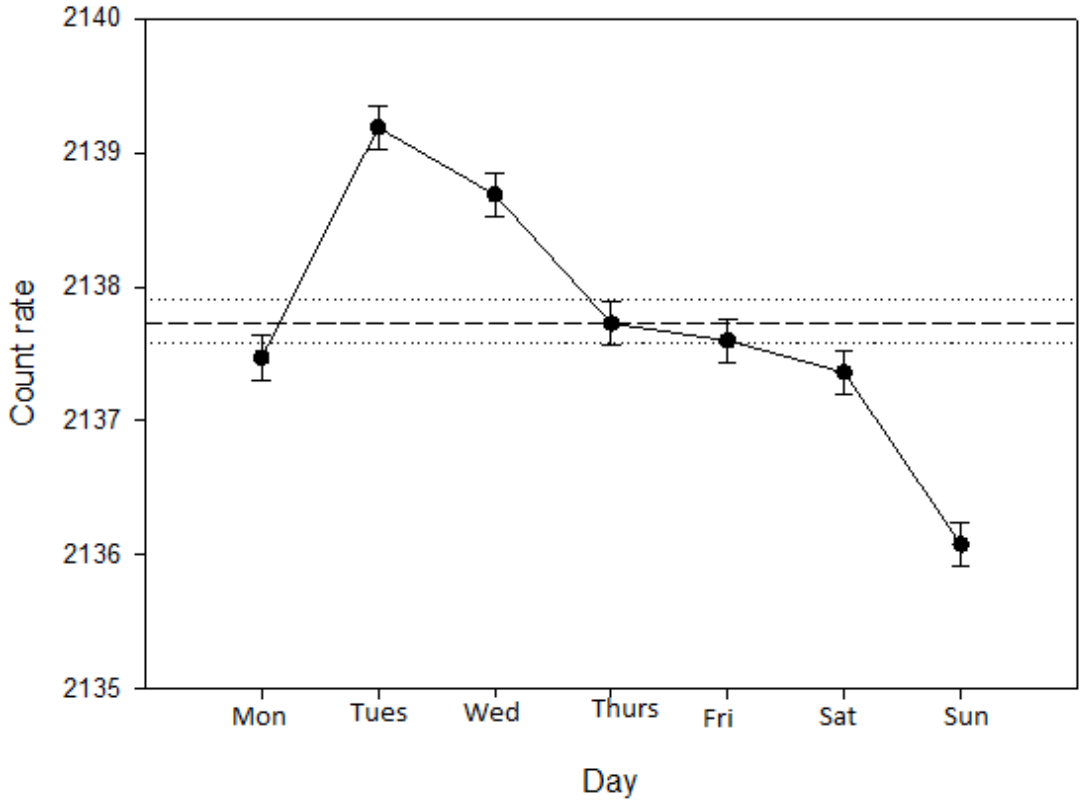

Figure 7 Daily count rates of ^{60}Co with reference line for the mean and statistical error of the mean

Figure 7 shows the count rates for each day over the week that the data was collected with reference lines representing the mean and the statistical uncertainty of the measurement. Only Monday, Thursday and Friday's measured count rates are found within two σ of the mean, with Thursdays count rate equal to the mean. The figure shows an increase in the count rates on Tuesday and Wednesday potentially due to the amount of human activity in the building in which the detector is located. The graph also shows a reduced count rate on Sunday. The count rate on the Thursday was found to be, 2173.73 counts per second, the same value as the mean of the entire week with Friday being within the error of this value. The Tuesday, Wednesday and Sunday decay rates were considerably different to those of the rest of the week and were 8.84, 5.41 and 10.04 σ away from the mean respectively. The statistical uncertainty of the count rates amounts to 0.008% of the values calculated. The decay rates are expected to drop throughout the week as the nuclei of the sample decay reducing the number of nuclei available to decay. The early morning Monday data was collected at the end of the week-long data collection period which explains the jump in count rates between Monday and Tuesday.

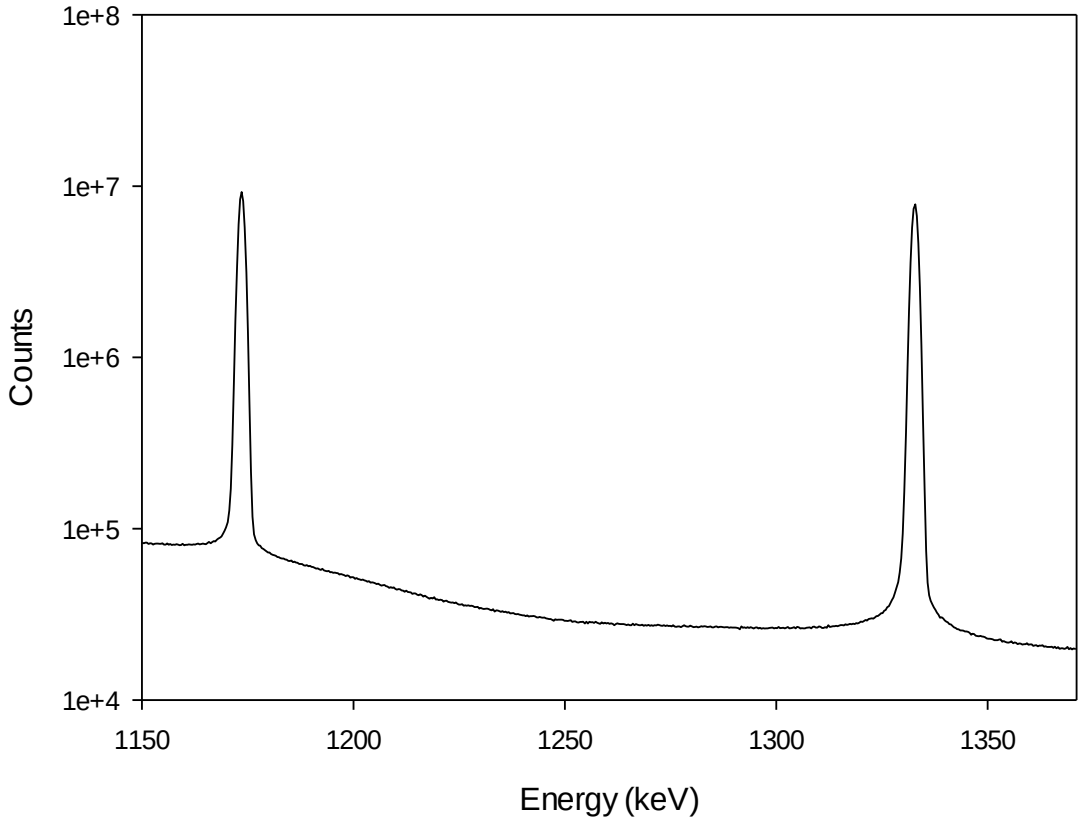

Figure 8 The energy correlated spectrum of the 1170-1371 keV energy window

In order to limit the influence of background radiation and to prevent misidentification of events further analysis was done on the 450 channels (3235-3685 corresponding to 1170-1371 keV) that include the two full energy peaks at 1173 and 1332 keV (see figure 8). The count rates of these two peaks will be taken and analysed again separately with all the counts detected assumed to correspond to a single decay. The statistical error is again calculated using $\sigma = \frac{\sqrt{Total\ decays\ (1170-1371\ keV)}}{Live\ time}$.

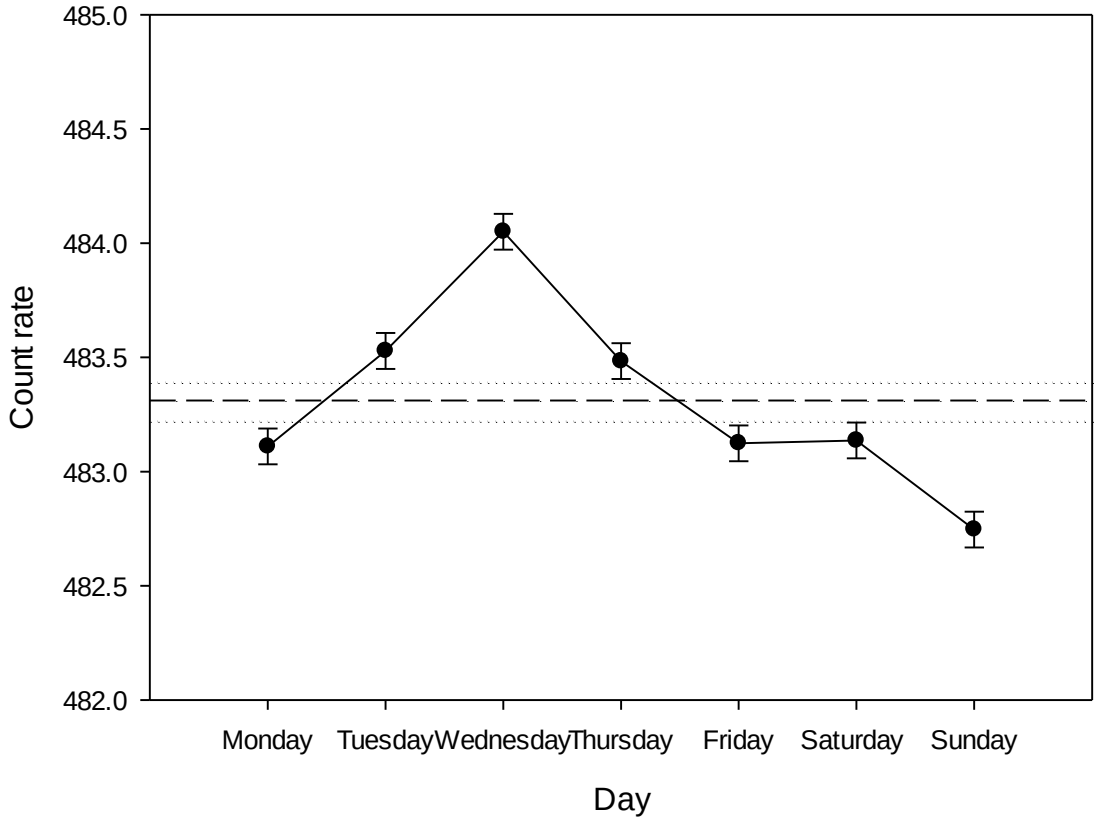

Figure 9 The daily count rates found within the 1170-1371 keV energy window.

Table 2 Daily count rates in 1170-1371 keV energy window

Day	Peak Count Rate	Uncertainty	Relative Uncertainty (%)
Monday	483.10	0.08	0.016
Tuesday	483.52	0.08	0.016
Wednesday	484.05	0.08	0.016
Thursday	483.48	0.08	0.016
Friday	483.12	0.08	0.016
Saturday	483.13	0.08	0.016
Sunday	482.74	0.08	0.016

Figure 9 shows the change in the daily count rates for the energy window with the mean and error bars included as reference lines. The graph now shows four of the days are below the mean count rate with three above. The count rates of the reduced spectrum follow a similar pattern to those of the full spectrum but with far less variability between days. Although unexpectedly with a higher activity on Wednesday as opposed to Tuesday. The statistical uncertainty in the measurements decreases due to fewer counts being measured. There is only a 0.27% difference between the highest and lowest rates, when looking at the entire spectra there is only a difference of 0.14%. The relative uncertainty of the count rates was found to increase to 0.016%, 2.1x the relative uncertainty when looking at the entire spectrum although this is expected due to the decreased number of counts in the reduced

spectrum. A mean of the decay rates was taken and found to be 483.311 decays per second. Each of the daily count rates are now outside 2 σ from the mean, with Tuesday the highest at 9.4 σ and Thursday the smallest with 2.2 σ. Focussing on the energy window has reduced the size of the more extreme outliers, now only two days have count rates over 2.8 σ from the mean whereas when looking at the entire spectra there were three. From this data it would be expected that the hourly decay rates would show a similar pattern of higher count rates during the typical working hours of 9 to 5 and reduced count rates outside these hours.

To view whether the count rates vary on a day to day basis the count rates for the full spectra will be corrected for the decays undergone throughout the measurement. To do this the textbook value of λ for ^{60}Co is used to calculate $e^{-\lambda t}$, from the exponential decay law, to include the decrease in count rate due to decays. For a single day this value is 0.99964. The count rate for Monday will not be included in this correction due to half of the hourly count rates being collected a week after the first as the data collection began in the late morning.

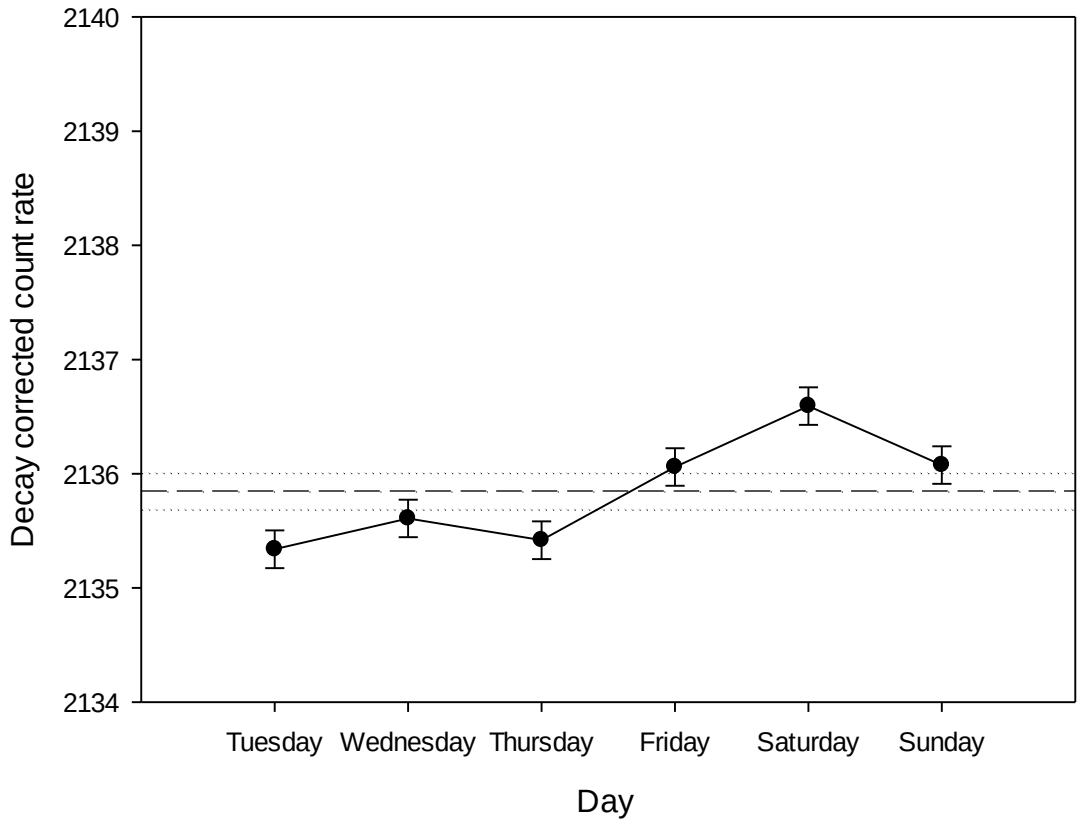

Figure 10 The decay corrected daily count rates with reference lines for the mean and statistical uncertainty

Figure 10 shows how the decay correction removes the large changes throughout the week and shows an increased activity over the weekend which was not observed in the non-corrected data. The error bars of three of the days count rates are within 2σ of the mean. The mean value of the count rates was found to be 2135.85.

4.2 Hourly Variability

Once again, the count rates for the entire spectrum were analysed first. The table shows a similar pattern to what was expected with increased counts throughout the typical work hours.

Table 3 Hourly count rates with uncertainty and relative uncertainty

Time	Count Rate	Uncertainty	Relative Uncertainty (%)
00:30	2137.93	0.81	0.04
01:30	2137.50	0.81	0.04
02:30	2137.22	0.81	0.04
03:30	2137.36	0.81	0.04
04:30	2136.83	0.81	0.04
05:30	2137.46	0.81	0.04
06:30	2137.24	0.81	0.04
07:30	2137.75	0.81	0.04
08:30	2137.34	0.81	0.04
09:30	2137.51	0.81	0.04
10:30	2137.63	0.81	0.04
11:30	2137.98	0.81	0.04
12:30	2138.32	0.81	0.04
13:30	2138.62	0.81	0.04
14:30	2138.38	0.81	0.04
15:30	2138.34	0.81	0.04
16:30	2138.71	0.81	0.04
17:30	2137.88	0.81	0.04
18:30	2137.62	0.81	0.04
19:30	2137.44	0.81	0.04
20:30	2137.78	0.81	0.04
21:30	2137.90	0.81	0.04
22:30	2137.25	0.81	0.04
23:30	2137.76	0.81	0.04

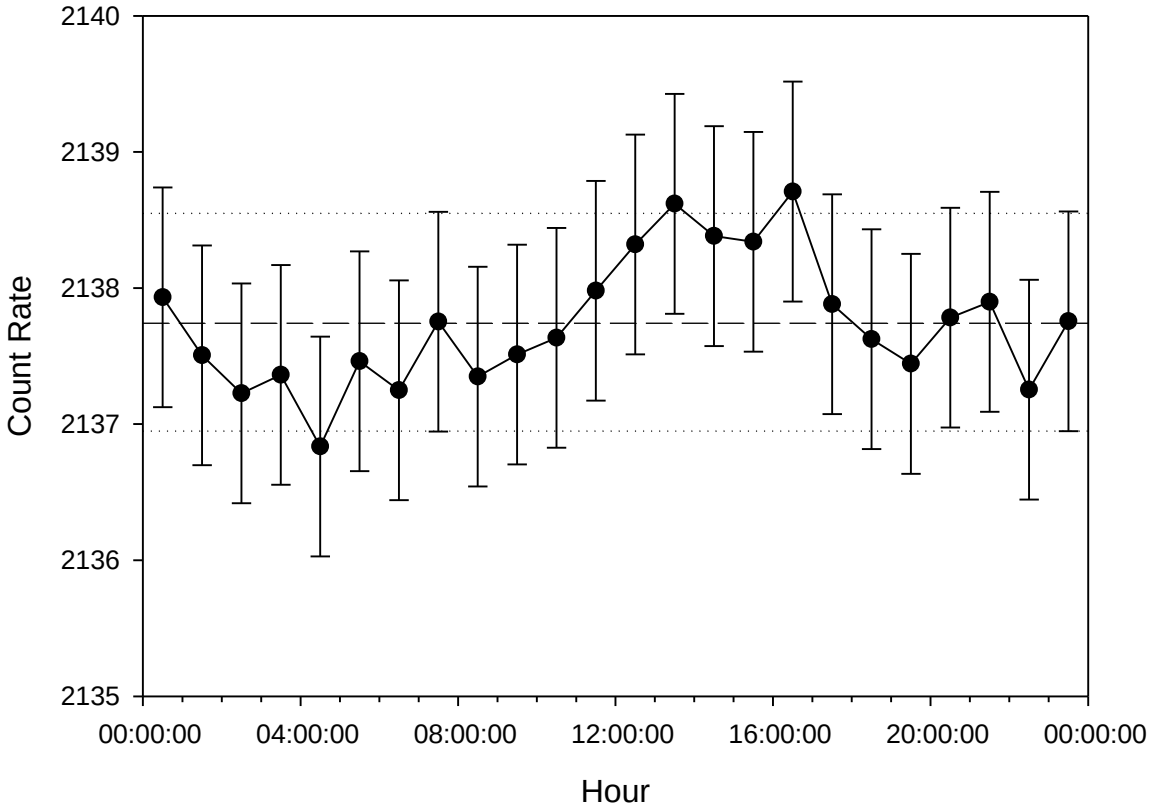

Figure 11 Hourly count rates over 24 hours with reference lines for mean with statistical uncertainty

The σ values were calculated and used as error bars on the graphs. For these measurements the background radiation would correspond to 1.5σ so would not be statistically significant. Due to the much shorter counting times the error bars are significantly larger. Figure 11 shows the change in count rates over a 24-hour period. The figure shows only the decay rates at 4:30, 13:30, 16:30 are found to be over one σ away from the mean count rate for the full 24 hours. The graph shows increased count rates during working hours but as most of the count rates are within one σ of the mean this is likely to be due to counting statistics. In the hourly measurement the statistical uncertainty was found to be 0.81 with the relative uncertainty 0.04% of the measured count rates.

Once again, the 1170-1371 keV energy window was analysed separately. This reduces the total number of counts and therefore reduces the value of σ and also the relative uncertainty down to 0.03%. The number of hourly count rates that are outside one σ difference is found to increase. As seen in figure 12 three of the hourly values now exceed two σ from the mean, those are 4:30, 12:30 and 13:30. A further ten hourly count rates now exceed one σ from the mean. This highlights the large variation in the measured decay rates. As these count rates are measured over a week the pattern of the variation observed here may not continue over a longer time frame.

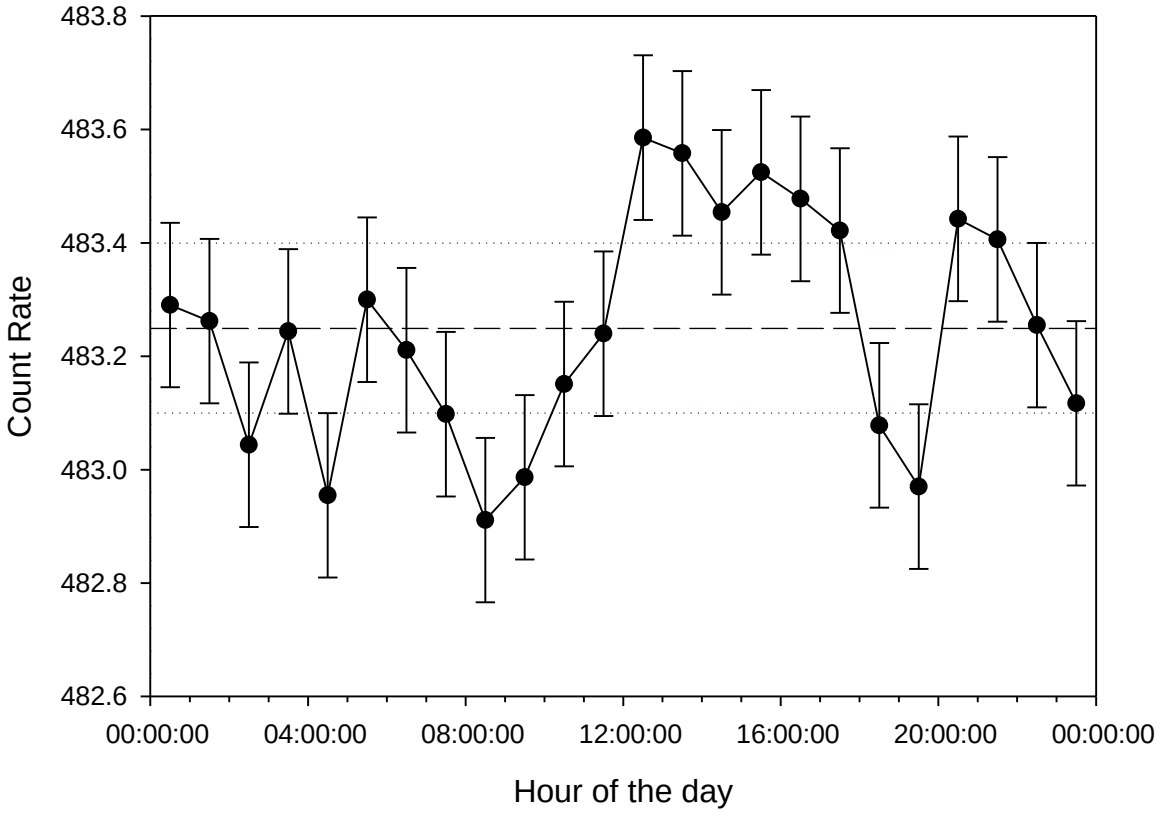

Figure 12 Hourly count rates of ^{60}Co between 1170-1371 keV with reference lines showing the mean with statistical uncertainty

Table 4 Hourly count rates between 1170-1371 keV with uncertainty and relative uncertainty

Hour	Count Rate (1170-1371 keV)	Uncertainty	Relative Uncertainty (%)
00:30	483.29	0.15	0.03
01:30	483.26	0.15	0.03
02:30	483.04	0.15	0.03
03:30	483.24	0.15	0.03
04:30	482.30	0.15	0.03
05:30	483.30	0.15	0.03
06:30	483.21	0.15	0.03
07:30	483.10	0.15	0.03
08:30	482.91	0.15	0.03
09:30	482.99	0.15	0.03
10:30	483.15	0.15	0.03
11:30	483.24	0.15	0.03
12:30	483.59	0.15	0.03
13:30	483.56	0.15	0.03
14:30	483.45	0.15	0.03
15:30	483.52	0.15	0.03
16:30	483.48	0.15	0.03
17:30	483.42	0.15	0.03
18:30	483.08	0.15	0.03
19:30	482.97	0.15	0.03
20:30	483.44	0.15	0.03
21:30	483.40	0.15	0.03
22:30	483.25	0.15	0.03
23:30	483.12	0.15	0.03

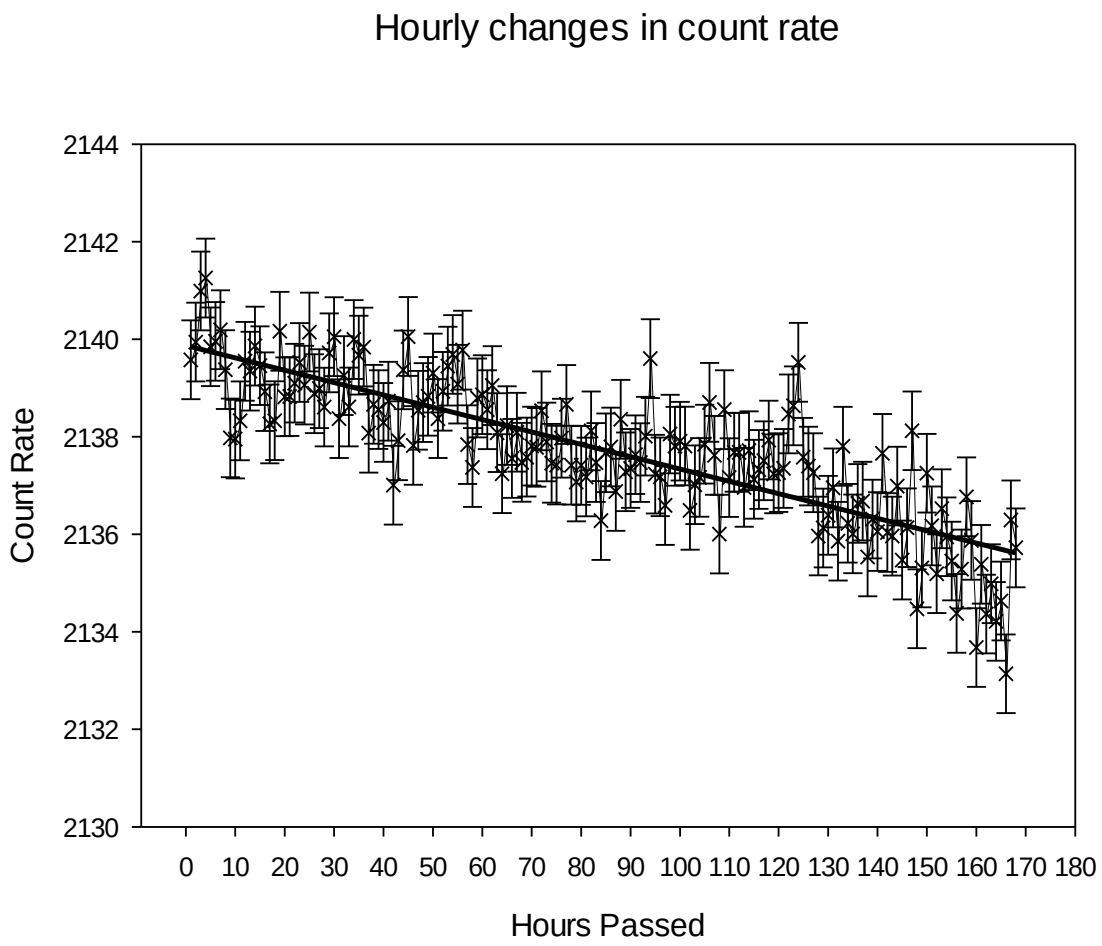

Figure 13 Hourly count rates over 168 hours with a trend line

Figure 13 above shows the count rate of the source per hour over the whole data collection period. There is an overall downward trend, with a slope of -0.025. The trend line has an r value of -0.83 which corresponds to a strong negative correlation between the data and the trend line. This relationship is expected due to the decay rate being proportional to the number of nuclei left which declines as nuclei decay in accordance with the exponential decay law. Taking the textbook value of the decay constant of ^{60}Co as $\lambda=0.131527$ years^{-1} and the 7 days over which the measurement is taken would lead to the count rate to decrease by a factor of 0.00251926 by the end of the week.

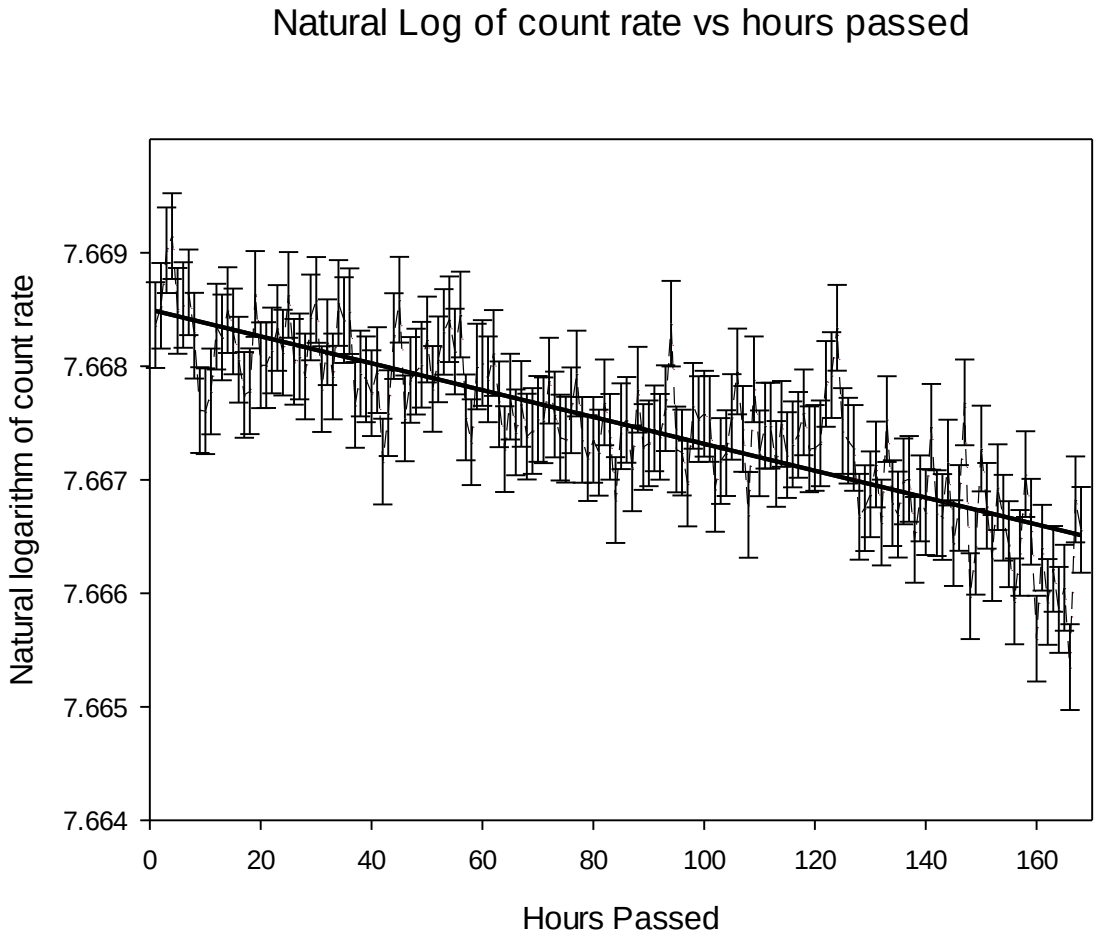

Figure 14 The natural logarithm of the hourly count rates over the 168 hours of measurement

The natural log of the count rate gives $ln\left(\frac{dN}{dt}\right) = ln(\lambda N_0) - \lambda t$. Plotting the natural logarithm of the count rate as a function of time (Figure 14) enables us to calculate the lambda from the slope. The uncertainty in the natural log of the count rate is given by $\Delta Ln(x) = \frac{\Delta x}{x}$ where *x* is the count rate. This gives a relative uncertainty of 0.00429%. The data collected is shown to vary either side of the trend line. The slope of the trend line finds λ=0.10309 years^{-1} with r=- 0.83. With the textbook value λ=0.131527years^{-1} the value found in this experiment is therefore 22% less than the true value. This is due to the small size of the decay constant and the short duration of the measurements resulting in large error bars due to statistical uncertainty. If the duration of the measurement was increased it is likely to supply a closer value.

4.3 Position

As semiconductor gamma spectrometers use a crystal the sample is placed on top of the detector therefore there is a possibility that the alignment and positioning of the source could affect the count rates measured. To test this, spectra were taken over a 24-hour period in the alignment used for the daily and hourly measurements once this was taken the source was rotated through 90 degrees and a 24-hour spectrum was taken again. Figure 15 below shows the orientations of the positions within the detector. Each position had two sets of measurements, once directly after the spectrometer was opened and again directly after the first measurement. This enabled a direct comparison of the count rate observed with the sample under conditions as similar as possible, with the first measurement providing the count rates to use as a comparison. The measurements were repeated every 90 degrees until the sample had rotated through a full 360 degrees.

Figure 15 The detector on which the source is placed with numbers relating to the different positions measured

This data was again entered into Microsoft Excel and the measurements for each position are compared. After calculating the statistical error in the measurements, the variation of the count rates can be used to calculate a potential variation in λ. In order to find any potential change in the lambda values the count rates of the two measurements, the first is divided by the second giving the following $\frac{Count\ rate\ 1}{Count\ rate\ 2} = \frac{\lambda e^{-\lambda t}}{\lambda e^{-\lambda(t+\tau)}}$ where τ is the time difference between the first and second measurements. This formula reduces to $\frac{Count\ rate\ 1}{Count\ rate\ 2} = \frac{\lambda_1}{\lambda_2 e^{-\lambda\tau}}$. The error propagation is given by $\frac{\sigma(\frac{cr1}{cr2})}{(\frac{cr1}{cr2})} = \sqrt{\left(\frac{\sigma\ count\ rate\ 1}{count\ rate\ 1}\right)^2 + \left(\frac{\sigma\ count\ rate\ 2}{count\ rate\ 2}\right)^2}$. As λ is very small for Co^{60} the first analysis will take $e^{-\lambda t} = 1$.

Table 5 Two count rate measurements for four separate positions with uncertainty

Position	Measurement	Count Rate	Uncertainty	Relative Uncertainty (%)
1	First	2127.55	0.17	0.008
	Second	2126.64	0.17	0.008
2	First	2131.03	0.17	0.008
	Second	2130.30	0.17	0.008
3	First	2119.89	0.17	0.008
	Second	2119.79	0.17	0.008
4	First	2112.55	0.17	0.008
	Second	2126.64	0.17	0.008

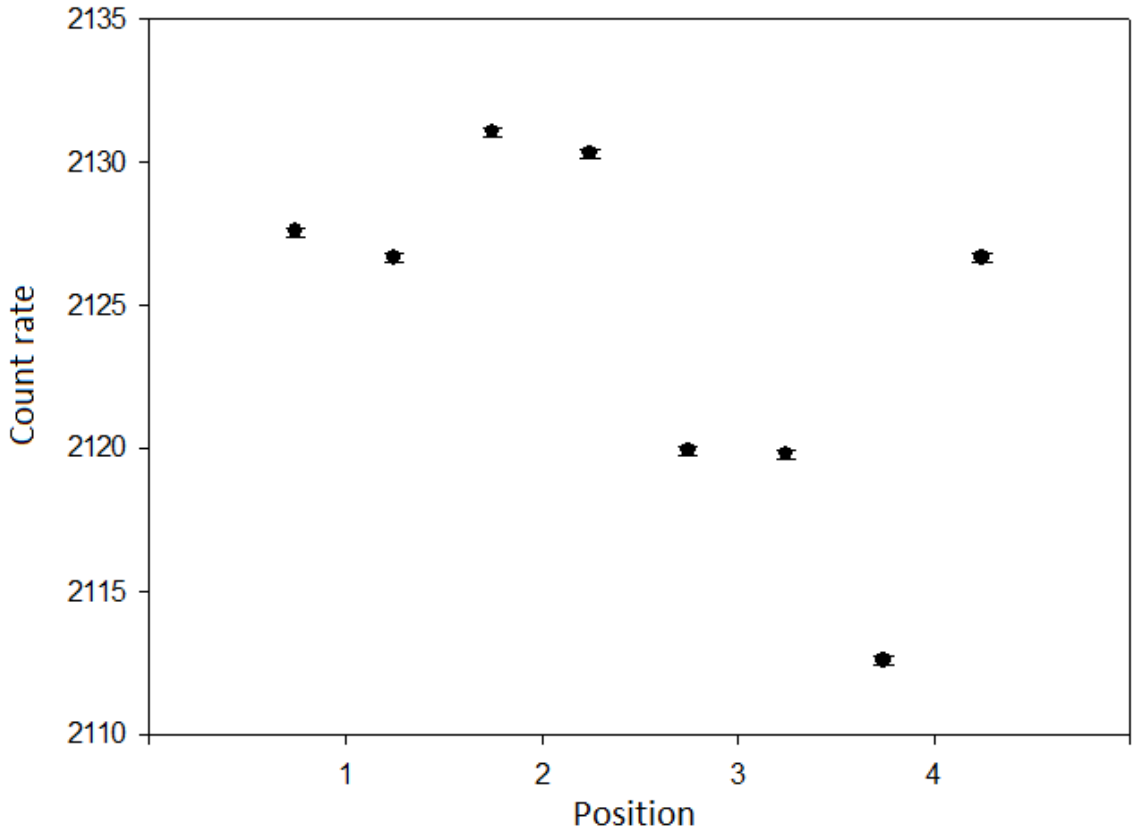

Figure 16 Graph showing the two count rates measured for each position.

Figure 16 shows the variation in the count rates between each measurement with the statistical uncertainty as the error bars. The difference in count rate between each measurement for each of the position exceeds the statistical error, except in position 3 which there is only a 0.62σ difference. Position 4 has the largest deviation with a difference of almost 85σ between the count rates of each measurement. The two measurements for position 4 were taken on a Friday and Saturday which may explain the increase in count rate as when corrected for decays the daily count rate measurements found increased activity

on Saturday compared to Friday although this increase in activity does not seem to be high enough to explain this difference.

Once again, the 450 channels covering the 1170-1371 keV energy window are analysed separately.

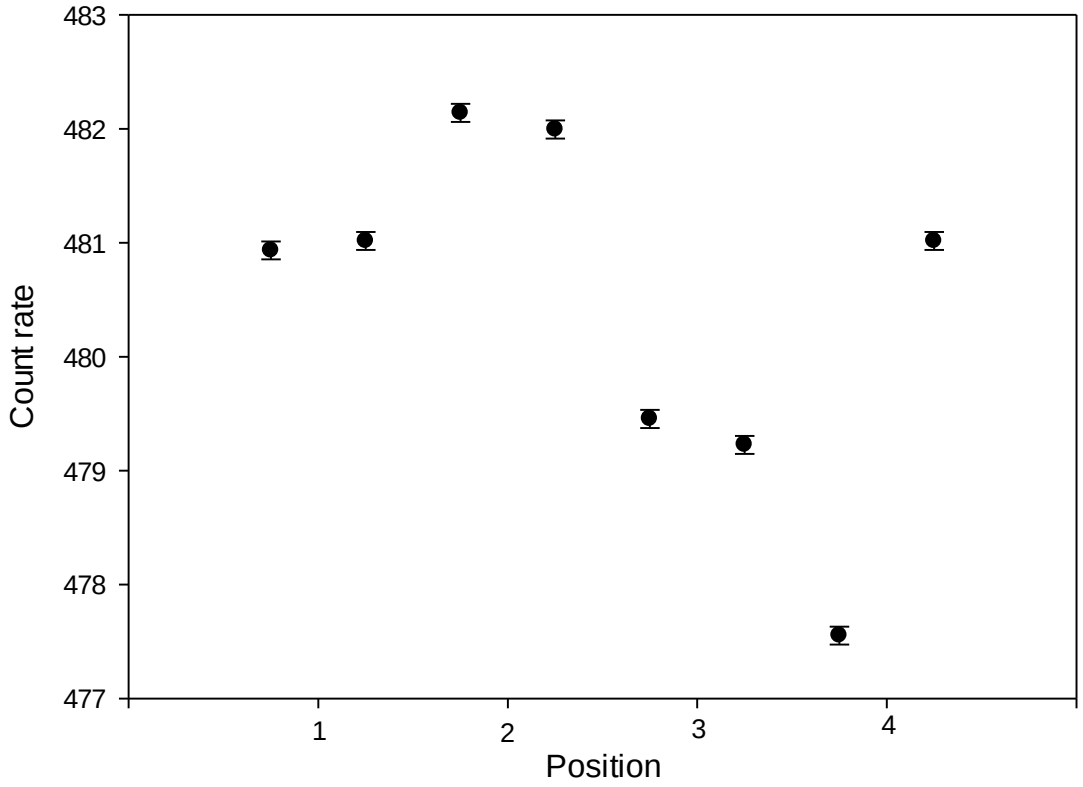

Figure 17 Count rates covering the 1170-1371 keV energy window for each positioning

Table 6 The count rates measured for the 1170-1371 keV energy window with uncertainties

Position	Measurement	Count rate	Statistical uncertainty	Relative uncertainty (%)
1	First	480.94	0.08	0.017
	Second	481.02	0.08	0.017
2	First	482.14	0.08	0.017
	Second	481.99	0.08	0.017
3	First	479.45	0.08	0.017
	Second	479.23	0.08	0.017
4	First	477.55	0.08	0.017
	Second	481.02	0.08	0.017

Figure 17 above shows the changes in count rate measurements between the two measurements the source underwent. The difference between each measurement in respect to σ has increased for all positions except position 4. Position 4 has a 43.88σ increase in count rate between the first and second measurements. This increase may be

due to the day on which the spectra were collected as position 4 was first measured on a Friday and had the second measurement on Saturday, which has an increased activity according to the time corrected daily count rates. The count rates of positions 2 and 3 both decreased with the count rate of position 2 dropping by 1.838σ or 0.030%, and position 3 by 2.877σ or 0.047% close to the 0.036% predicted by the exponential decay law. The count rate for position 1 increases by exactly 1σ. This increase is unexpected as the count rate for the entire spectrum decreases.

Table 7 The ratio of count rates measured for each position with relative uncertainty

Position	cr_1/cr_2	Sigma cr_1/cr_2 (%)
1	1.000	0.011
2	1.000	0.011
3	1.000	0.011
4	0.993	0.011

The error achieved amounts to a 0.011% change in the ratios of count rates, any changes measured smaller than this may be due to statistical effects.
If we now take the textbook value of λ to calculate $e^{-\lambda t}$ to correct for the change in count rate due to the decay of nuclei, for a single day this value is 0.999639717, so the count rate of the first measurement will be multiplied by this in order to calculate the ratios with decay correction.

Table 8 Ratio of full spectra count rates for the first and second measurements with decay correction and relative uncertainty

Position	Measurement	Count rates with decay correction	cr_1/cr_2 with decay correction	Sigma cr_1/cr_2 (%)
1	First	2126.79	1.000	0.011
	Second	2126.64		
2	First	2130.27	0.999	0.011
	Second	2130.29		
3	First	2119.13	0.999	0.011
	Second	2119.79		
4	First	2111.79	0.993	0.011
	Second	2126.64		

This error is found to be the same as without the decay correction as neither the number of decays measured nor the live time of detection are affected by this correction.
As with the previous analysis this will be done again on the energy window containing the two most prominent decay peaks to see whether it is possible to achieve a more accurate ratio an in an attempt to remove background gammas and reduce the error.

Table 9 Ratio of count rates and relative uncertainty for 1170-1371 keV energy window

Position	cr_1/cr_2	Sigma cr_1/cr_2 (%)
1	0.999	0.02
2	1.000	0.02
3	1.000	0.02
4	0.993	0.02

When only using the data from the peaks it appears to have increased the error in the ratios compared to when using the entire spectrum, the error in this calculation means that only a change in of over 2% will exceed the statistical variation.
Once again, the count rates will be corrected for decay and the count rate ratios calculated again.

Table 10 Count rate ratios with decay corrections for energy window 1170-1371 keV

Position	Measurement	Count Rates with decay correction	cr_1/cr_2 with decay corrections	Sigma cr_1/cr_2 (%)
1	First	480.94	0.998	0.02
	Second	481.02		
2	First	481.97	0.999	0.02
	Second	481.99		
3	First	479.28	1.000	0.02
	Second	479.23		
4	First	477.38	0.992	0.02
	Second	481.02		

When analysing the reduced spectra there are much more pronounced variations between the count rates of the measurements, although this is also counteracted by the increase in uncertainty. This results in a less accurate and precise measurement of any possible variation in the count rates and thus also any potential λ measurement.

6. Discussion

Further analysis is required to find the smallest change in λ detectable with a 0.01% change in the ratio of count rates. To do this the formula of the count rates of the two samples both before and after exposure will need to be derived from the exponential decay law. Before exposure the count rates for the first sample will be given by $r_1 = \frac{\partial N_1(t)}{\partial t} = -\lambda N_1(0)e^{-\lambda T_1}$ with the second sample being given by $r_2 = \frac{\partial N_2(t)}{\partial t} = -\lambda N_2(0)e^{-\lambda T_2}$ where T_1 and T_2 represent the time of the measurement before exposure for the first and second sample respectively. This gives the pre exposure ratio of count rates as $R_{PE} = \frac{r_1}{r_2} = \frac{\lambda N_1(0)e^{-\lambda T_1}}{\lambda N_2(0)e^{-\lambda T_2}} = \frac{N_1(0)}{N_2(0)}e^{-\lambda(T_1-T_2)}$. To find the formula for the post exposure decay rates the exposure time needs to be defined as ΔT. For the sake of convenience, it also helps to take $T_{2,AE}=T_2+\Delta T$ where $T_{2,AE}$ is the duration of the post exposure measurement for the second sample and $T_{1,AE}$ is the after-exposure measurement duration for the first sample. This results in the following formulae for the post exposure count rates

$r_{1,AE} = \frac{\partial N_1(t)}{\partial t} = \lambda N_1(t) = \lambda N_1(0) e^{-\lambda T_{1,AE}}$ and
$r_{2,AE} = \frac{\partial N_2(t)}{\partial t} = \lambda N_2(t) = \lambda N_2(0) e^{-\lambda T_2} e^{-(\lambda+\Delta\lambda)\Delta T} = \lambda N_2(0) e^{-\lambda T_{2,AE}} e^{-\Delta\lambda\Delta T}$.
This gives the ratio of after exposure count rates as
$R_{AE} = \frac{r_{1,AE}}{r_{2,AE}} = \frac{\lambda N_1(0) e^{-\lambda T_{1,AE}}}{\lambda N_2(0) e^{-\lambda T_{2,AE}} e^{-\Delta\lambda\Delta T}} = \frac{N_1(0)}{N_2(0)} e^{-\lambda(T_{1,AE}-T_{2,AE})} e^{\Delta\lambda\Delta T}$.
To isolate $\Delta\lambda$ the ratio of pre-exposure and after exposure ratios is needed, this is given by the following equation

$$\frac{R_{PE}}{R_{AE}} = \frac{\frac{N_1(0)}{N_2(0)} e^{-\lambda(T_1-T_2)}}{\frac{N_1(0)}{N_2(0)} e^{-\lambda(T_{1,AE}-T_{2,AE})} e^{\Delta\lambda\Delta T}} = \frac{e^{-\lambda(T_1-T_2)}}{e^{-\lambda(T_{1,AE}-T_{2,AE})}} e^{-\Delta\lambda\Delta T}$$

This can be simplified by taking T_1-T_2 =$T_{1,AE}$-$T_{2,AE}$ this reduces the formula to $\frac{R_{PE}}{R_{AE}} = e^{-\Delta\lambda\Delta T} \Rightarrow \Delta\lambda = -\frac{1}{\Delta T} \ln \frac{R_{PE}}{R_{AE}}$
In order to find $\Delta\lambda$ in respect to the change in the count rate ratio the after-exposure ratio is given as R_{AE}= R_{PE}+ΔR.
This leads to $\Delta\lambda$ being given by the following $\Delta\lambda = -\frac{1}{\Delta T} \ln \frac{R_{PE}}{R_{PE}+\Delta R} = \frac{1}{\Delta T} \ln\left[1 + \frac{\Delta R}{R_{PE}}\right] \approx \frac{1}{\Delta T} \frac{\Delta R}{R_{PE}}$
This gives $\frac{\Delta\lambda}{\lambda} \approx \frac{1}{\lambda\Delta T} \frac{\Delta R}{R_{PE}}$. This formula shows that the accuracy of the measurement of a change in the decay constant depends on the decay constant being tested as well as the length of exposure of the tested sample. In the case of this thesis the sample is assumed to undergo a year long exposure. The λ for ^{60}Co is 0.132 year^{-1} this gives $\frac{\Delta\lambda}{\lambda} \approx 7.57 \frac{\Delta R}{R_{PE}}$. With a 24-hour measurement of the decay rate of ^{60}Co the uncertainty in the count rate ratios was found to be $\frac{\Delta r}{r} = 0.011$ for the full spectrum The uncertainty in the ratio of ratios is then given as $\frac{\delta R}{R} = \sqrt{(\frac{\Delta r_1}{r_1})^2 + (\frac{\Delta r_2}{r_2})^2}$ which results in $\frac{\Delta R}{R_{PE}}$=0.016.
Therefore, the minimum achievable uncertainty would be $\frac{\Delta\lambda}{\lambda} = 0.11\%$. For the 1170-1371 keV energy window $\frac{\Delta r}{r} = 0.022$ which when using $\frac{\delta R}{R} = \sqrt{(\frac{\Delta r_1}{r_1})^2 + (\frac{\Delta r_2}{r_2})^2}$ results in an uncertainty in the ratio of count rate ratios of $\frac{\Delta R}{R_{PE}}$=0.0311. Which results in a relative error in the measurement of $\frac{\Delta\lambda}{\lambda} = 0.24\%$.

Using this formula, it is possible to calculate the change in λ due to the changing of the alignment of the source. As the sources used were not exposed an exposure period of 1 year will be presumed. For the full spectrum there were changes in the ratio of count rate ratios ($\frac{\Delta R}{R}$) of 0.001 and 0.007. If these changes were observed after a year long exposure of the source they would correspond to a $\frac{\Delta\lambda}{\lambda}$ of 0.008% ± 1.2x10^{-6} for a 0.001 change in count rate ratio and a $\frac{\Delta\lambda}{\lambda}$ of 0.053% ± 8.5x10^{-6} for the 0.007 change. For the 1170-1371 keV energy window there were changes of 0.001, 0.002 and 0.008 in the ratio of count rate ratios, these correspond to $\frac{\Delta\lambda}{\lambda}$ of 0.008% ± 1.8x10^{-5}, 0.016% ± 3.6x10^{-5} and 0.06% ± 1.5x10^{-4} respectively. The actual uncertainty in this measurement is much higher due to the lack of exposure time of the sources.

The achievable accuracy could be increased by increasing the exposure time of the tested sample doubling the time of exposure would halve the relative uncertainty in the measurement of $\Delta\lambda$. A further change that could be made is to use a radionuclide with a larger decay constant value. This would reduce the uncertainty in λ in relation to the uncertainty in the count rate ratios. Without an increase in the detection time the increased activity of the source will lead to an increased statistical uncertainty in the measurement of the count rate ratios, however the increased number of events detected is likely to reduce the relative uncertainty. In order to find the most accurate measurement of $\Delta\lambda$ the statistical uncertainty in the count rate measurements needs to be minimised. Currently the relative uncertainty in the decay rates ranges from 0.0077- 0.0377%. 0.0077% is one order larger than the 0.0023% uncertainty found in literature (Pomme et al 2018). In addition to reducing the error in the count rates by increasing the time period over which the experiment runs would also provide a chance to observe potential seasonal variations.
The changes in the count rate between positions may be due to the days of measurement. As a variation was observed in the weekly and hourly measurements this variation is likely to have affected the different position measurements.
These variations could be caused by radon, a naturally radioactive gas of which 48% of background radiation is attributed to by the World Nuclear Association. This could explain the daily differences in decay rates over the week as human activity will affect the amount of radon in the room containing the detector. In order to check whether this is the case it is important to look at the decay scheme of radon. Radon itself does not produce any gamma photons but its decay products do, ^{214}Bi produces 45% of its gamma photons at energies of 609 keV. If peaks are found at this energy in the spectrum it can be assumed that some of the variation in decay rates could be attributed to this, although this would not feature in the analysis of the 1170-1371 keV energy window. There were no peaks found in the spectra so any variations in the decay rate measured cannot be attributed to background radon radiation and therefore must be from other sources.
The primary way to improve the accuracy of the experiment would be to increase the live time of the detections, this would reduce the statistical uncertainty of the measurements. Using a stronger source of ^{60}Co would also increase the number of events detected which would in turn reduce the relative uncertainty due to counting effects by a factor of $\frac{1}{\sqrt{Number\ of\ detected\ events}}$ if the total detection period is not affected. If using a semiconductor gamma detector an increased activity will also increase the dead time in the detector so this factor may not occur in reality.

7. Conclusion

In this experiment a relative uncertainty of 0.011% in the count rate ratios was achieved for a 24-hour measurement with the full spectrum this is less than half the largest relative uncertainty achieved in literature (Pomme et al, 2018) but is still 2 orders larger than the smallest uncertainty obtained in that analysis. For the 1170-1371 energy window this increased to 0.02% uncertainty, the same as the largest uncertainty in the Pomme et al (2018) study. For a ^{60}Co sample with an exposure time of one year this enables a minimum relative uncertainty in $\Delta\lambda$ of 0.11% for the full spectrum due to statistical uncertainty and 0.24% was achieved for the 1170-1371 keV energy window. Using the change in ratios due to a change in positioning, with an assumed year long exposure a change in lambda in the

order of 10^{-3} is detectable. This accuracy could be increased by increasing the duration of the exposure of the tested sample or reducing the statistical uncertainty of the count rate ratio measurements. A radionuclide sample with a shorter half-life and therefore larger λ would reduce the uncertainty in the $\frac{\Delta\lambda}{\lambda}$ in relation to the achieved $\frac{\Delta R}{R}$. A stronger source would also reduce the relative uncertainty in the count rate measurements due to counting statistics.

8. References

Rutherford, E., Chadwick, J., & Ellis, C. (1931). *Radiations from Radioactive Substances* (Cambridge Library Collection - Physical Sciences). Cambridge University Press.

Jere H. Jenkins, Ephraim Fischbach, John B. Buncher, John T. Gruenwald, Dennis E. Krause, Joshua J. Mattes, Evidence of correlations between nuclear decay rates and Earth–Sun distance, Astroparticle Physics, Volume 32, Issue 1, 2009, Pages 42-46

DDEP, 2017. Table of Radionuclides. Monographie BIPM-5 (BIPM, Sèvres), Vol. 1–8 website: ⟨http://www.nucleide.org/DDEP_WG/DDEPdata.htm⟩.

Jere H. Jenkins, Ephraim Fischbach, Perturbation of nuclear decay rates during the solar flare of 2006 December 13, Astroparticle Physics, Volume 31, Issue 6, 2009, Pages 407-411,

S. Pommé, H. Stroh, T. Altzitzoglou, J. Paepen, R. Van Ammel, K. Kossert, O. Nähle, J.D. Keightley, K.M. Ferreira, L. Verheyen, M. Bruggeman, Is decay constant? Applied Radiation and Isotopes, Volume 134, 2018, Pages 6-12,

Reguigui, N 2006 Gamma Ray Spectrometry Practical Information Page 7

Physwiki ^{137}Cs spectrum

Nucleonica Reduced decay scheme of Cobalt 60